Int. J. Electrochem. Sci., 7 **(2012)** 2334 - 2348

International Journal of
ELECTROCHEMICAL
SCIENCE
www.electrochemsci.org

Electrochemical Corrosion Behaviour of Iron Rotating Disc Electrode in Physiological Medium Containing Amino Acids and Amino Esters as an Inhibitors

D. Bouzidi [1], *A. Chetouani* [1,2], *B. Hammouti* [1,*], *S. Kertit* [3], *M. Taleb* [4], *S.S. Al-Deyab* [5]

[1] LCAE-URAC18, Faculté des Sciences, Université Mohammed Premier, Oujda, Morocco.
[2] laboratoire de chimie physique, Centre Pédagogique Régional, Oujda, Morocco.
[3] Les Ecoles Arochd, Sale Aljadida, Morocco.
[4] Laboratoire d'Ingénierie des Matériaux, Modélisation et Environnement, Faculté des Sciences Dhar El Mahraz, Université Mohammed Ben Abdellah, Fès – Morocco
[5] Petrochemical Research Chair, Chemistry Department, College of Science, King Saud University, P.O. Box 2455, Riyadh 11451, Saudi Arabia
[*]E-mail: hammoutib@gmail.com

Received: 11 January 2012 / *Accepted:* 12 February 2012 / *Published:* 1 March 2012

The study of the corrosion of pure iron in physiological 9g/L NaCl medium was studied by electrochemical method under different hydrodynamic conditions. The hydrodynamic conditions were simulated by using a rotating disc electrode. The corrosion inhibition using amino acid, methionine, and some amino esters: methionine methyl ester and methionine ethyl ester, on the electrochemical behaviour of iron. The results showed that the criterion of Levich is proved. The limit current is function of the speed of rotation of the electrode of iron and process is a mixed type kinetic. On the electrochemical behaviour of iron is studied. The ethyl 2-amino-4-(methylthio) butanoate or methionine ethyl ester ($MetOC_2H_5$) is the best inhibitor of series and its effectiveness attains 80 % in 10^{-2}M. The $MetOC_2H_5$ acts on the iron surface according to the Frumkin model.

Keywords: Iron, Inhibition, Corrosion, Sodium chloride, rotating disk electrode.

1. INTRODUCTION

Iron or steel and its alloys have a low density, an attractive appearance, relatively good corrosion resistance and excellent thermal and electrical conductivity. The combination of these properties makes it a preferred choice for many industrial applications such as automobiles, food handling, containers, electronic devices, building, aviation [1-7], etc. Various attempts have been made to study the corrosion of iron or steel and its alloys, and their inhibition by organic inhibitors in acid

solutions and in physiological medium [8-14]. In physiological medium are used for pickling of iron and for its chemical or electrochemical etching. It can be important to add a corrosion inhibitor to decrease the speed of iron dissolution in such solutions. Thus, numerous studies concerning the inhibition of iron corrosion using organic substances have been conducted in physiological solutions [10, 11, 15-18]. Unfortunately, many common corrosion inhibitors are health hazards. To solve this problem, some researchers investigated the inhibition effect of amino acids and amino esters on corrosion of metals. These inhibitors are nontoxic, relatively cheap and easy to produce in purities greater than 99% [19-23]. The focus of this study is to investigate the inhibition properties of some amino acids and amino esters in physiological medium 9g/L of NaCl.

The adsorption of these molecules is influenced by their electronic structure, steric factors, aromaticity, electron density at the donor atoms, and p-orbital character of donating electrons [24-26]. The adsorption process is also affected by the presence of hetero atoms, such as N, O, P, and S as well as multiple bonds or aromatic rings in their molecular structure which are assumed to be active centres of adsorption. The adsorption of inhibitors takes place through heteroatoms. Generally, the tendency to form a stronger coordination bond and, as consequence, inhibition efficiency should increase in the order O<N<S<P [27-31]. Nitrogen-containing heterocyclic compounds are considered to be effective corrosion inhibitors. Several attempts have been made to predict corrosion inhibition efficiency with a number of individual parameters obtained via various quantum chemical calculation methods as a tool for studying corrosion inhibitors [2, 17, 32-36].

The effect of inhibitor concentration and temperature against inhibitor action was investigated. It was found that these inhibitors act as good inhibitors for the corrosion of lead alloy in physiological medium 9g/L. The behaviour of pure iron with and without inhibitor is studied using electrochemical method under different hydrodynamic conditions. Increasing inhibitor concentration increases the inhibition efficiency. It was found that adsorption of used amino acids on lead alloy surface follows Frumkin isotherm.

2. EXPERIMENTAL

2.1. Synthesis of the amino ester compounds

In the studied, the amino acid is product for analysis. The Chemical structure compound is presented below in Scheme 1.

The organic compounds amino esters tested as corrosion inhibitors were synthesized, purified and characterized by infra-red, ^1H nuclear magnetic resonance (NMR) spectroscopic methods and microanalysis before use. The synthesis method is as follows. at 0 °C in a flask fitted with a tube of $CaCl_2$ is added, drop wise, the mixture of amino acid (0.1 mol) and 100 ml of methanol, 8.5 ml of $S0Cl_2$.

The resulting mixture was stirred for 20 min at 0 °C, and then heated with stirring at room temperature for 2 hours. The reaction mixture is refluxed for 2 hours after adding a touch of hydroquinone. After cooling, the methanol is evaporated. The amino ester obtained is then washed

with ether and then filtered. The last operation is repeated four times to evaporate all of $SOCl_2$. The chemical formulas of amino esters studied are represented as follows in Scheme 2.

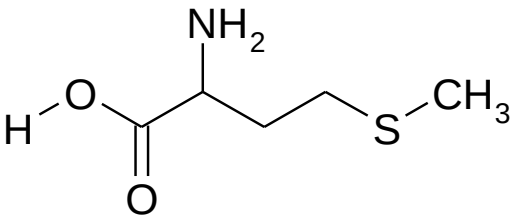

Methionine (MetOH)

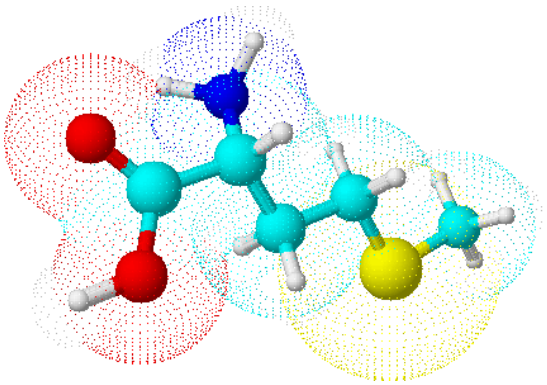

Scheme 1. Structure of amino acid inhibitor

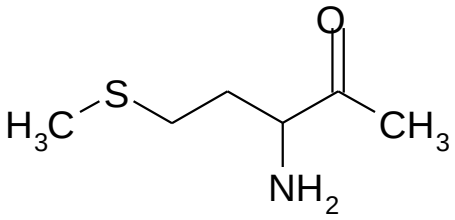

methyl 2-amino-4-(methylthio)butanoate
methionine methyl ester ($MetOCH_3$)

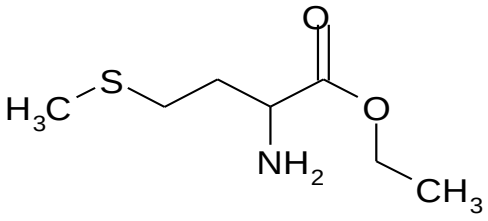

ethyl 2-amino-4-(methylthio)butanoate
methionine ethyl ester ($MetOC_2H_5$)

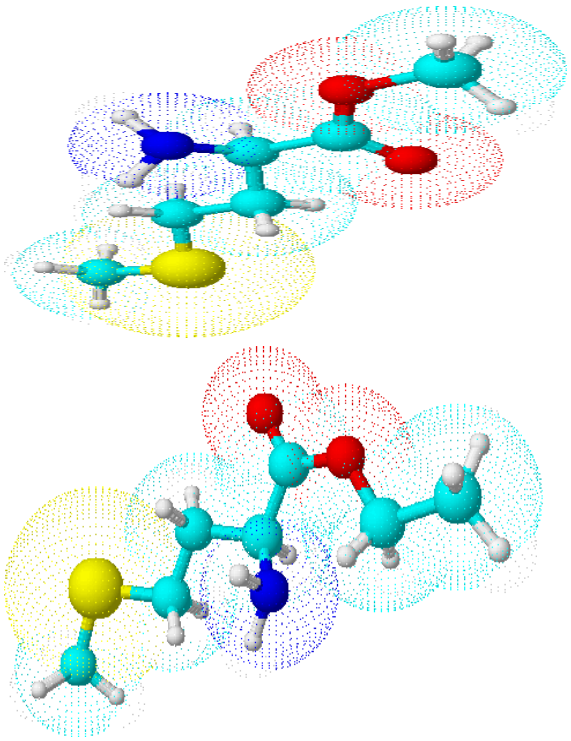

Scheme 2. Structure of amino ester inhibitors

2.2. Electrochemical measurements

The aggressive solution is physiological medium 9g/L was prepared with double-distilled water. Prior to all measurements, the pure iron samples used at 99.5% « Ref. LS99376 JV, Fe 00040, de Good Fellow, Angleterre ». the samples pure iron were polished with different emery paper up to

1200 grade, washed thoroughly with double-distilled water, degreased with AR grade ethanol, acetone and drying at room temperature.

Electrochemical measurements were carried out in a conventional three-electrode electrolysis cylindrical Pyrex glass cell. The working electrode (WE) is rotating disk (EDT), in the form of disc cut from pure iron has a geometric area of 0.31 cm^2, and is embedded in polytetrafluoroethylene (PTFE). A saturated calomel electrode (SCE) and a disc platinum electrode were used respectively as reference and auxiliary electrodes, respectively.

The temperature was thermostatically controlled at 310 ± 1 K. The WE was abraded with silicon carbide paper (grade P1200), degreased with AR grade ethanol and acetone, and rinsed with double-distilled water before use. The electrode potential was allowed to stabilize 60 min before starting the measurements. All experiments were conducted at 310 ± 1 K. Measurements were performed using Amel 449 Instrument Potentiostat. Tafel polarization curves were obtained by changing the electrode potential automatically from -1200 to -250 mV/SCE at open circuit potential with scan rate of 30 mV/mn^{-1}. The rotational speed of the electrode is fixed at 1000 rd / min.

Before recording the cathodic polarisation curves, the steel electrode is polarised at -800 mV for 10 min. For anodic curves, the potential of the electrode is swept from its corrosion potential after 60 min at free corrosion potential, to more positive values.

3. RESULTS AND DISCUSSION

3.1. Polarization curves in NaCl medium 9g /l only.

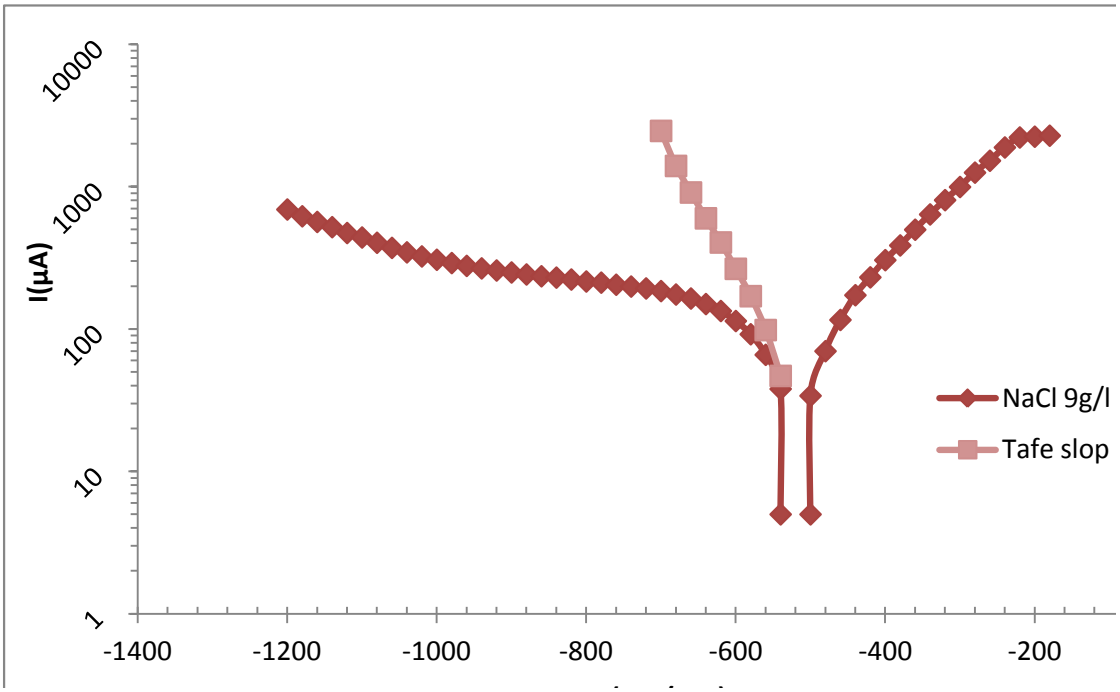

Figure 1. polarization curve of pure iron in 9g/L NaCl aerated at 310K.

To understand the mechanism of action of amino acid and amino esters, it is essential to study first the corrosion behaviour of iron in control medium in the absence of the inhibitor. The polarization curves were performed with a rotating disk electrode. The tests are performed in NaCl solution 9 g/l aerated at temperature 310K. The rotational speed of the electrode is fixed at 1000 rd/min.

The analysis showed the existence of a current platform, corresponding to the potential domain of -900 to -700mV, attributed to the oxygen diffusion. It is also because the individual anodic curve does not intersect the curve cathodic in the diffusion platform, but at the ascending part, the process is governed by electrochemical kinetics mixed activation-diffusion.

Note also that the cathode part can be subdivided into three domains. The first domain is characterized by an inflection point corresponding to a mixed kinetic (mass transfer + charge transfer). The second domain is the platform oxygen diffusion corresponds to the reduction reaction [37-39]. Where the value of the diffusion current is I = 758 $\mu A.cm^{-2}$.

$$2\ H_2O + O_2 + 4\ e^- \rightarrow 4\ OH^- \quad (1)$$

The third domain; begins at -1000mV/SCE. We observe a continuous increase of cathodic current. This phenomenon is related to the reduction of the solvent (H_2O) that results in a release of hydrogen, according to the reaction:

$$2\ H_2O + 2\ e^- \rightarrow 2\ OH^- + H_2 \quad (2)$$

In the domain anodic we are seeing an increase in the anodic current as a function of potential corresponds to the Tafel curve. We are therefore in the case of a pure activation. We conclude that iron is not passive in the potential range studied.

3.2. Effect of rotation speed on the polarization curves

Figure 2 shows the cathodic and anodic polarization curves at different rotation speeds. The change of rotational speed does not seem to affect the curves. They always show a platform, corresponding to the reaction of oxygen diffusion. However, the platform height increases with rotational speed. At each platform corresponds a limit diffusion current I_L.

Levich's relationship is verified [40], the current density diffusion limit I_L as a function of the square root of the rotation speed of the electrode is a straight line (Figure 3). We note also, that the right does not pass through the origin because there must be a non-diffusion current superimposed on the current i.e. $I = K + I_D$. This proves that the regime at the interface Fe / 9 ‰ NaCl is laminar hydrodynamic. Moreover, the measured currents in the cathodic domain, are affected by a diffusion and given by the following equation

$$\frac{1}{I} = \frac{1}{I_C} + \frac{1}{I_L} \quad \text{With } I_L = 0.62\ n\ F\ S\ X_0\ D_x^{2/3}\ \nu^{-1/6}\ w^{1/2}$$

I is the cathodic current measured in the kinetic mixed, I_c is the corrected current and limit diffusion current I_L with:

$$I_C = \frac{I_L * I}{I_L - I}$$

X_0 is the oxygen concentration, D_x is the oxygen diffusion coefficient, and w is the rotation speed

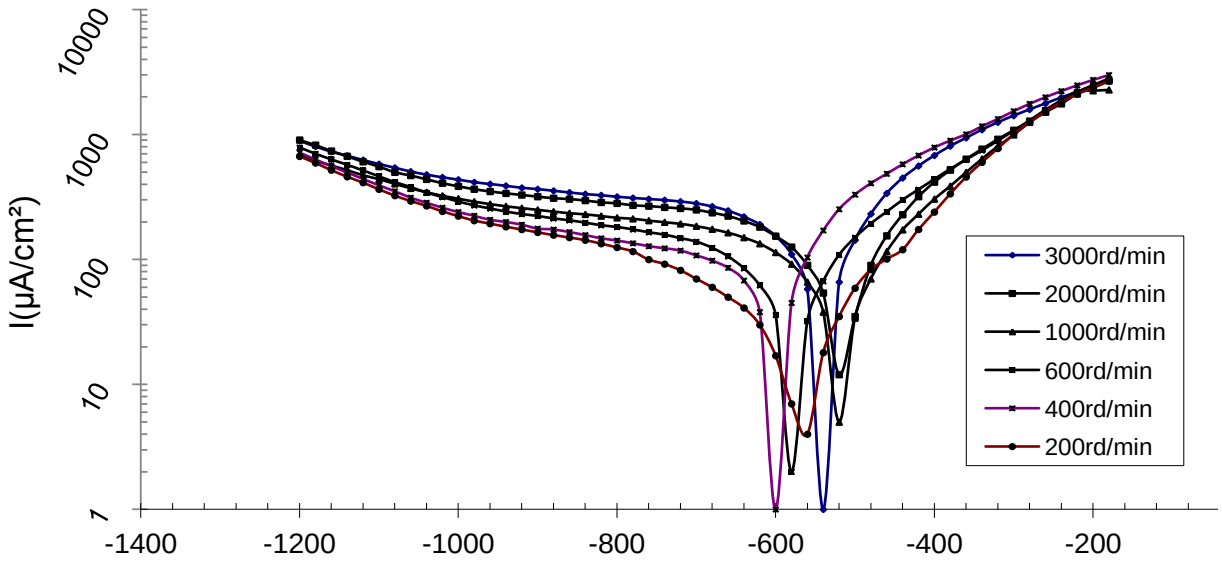

Figure 2. Effect of rotation speed on the IE curves of pure iron in 9g/l NaCl solution aerated at 310K.

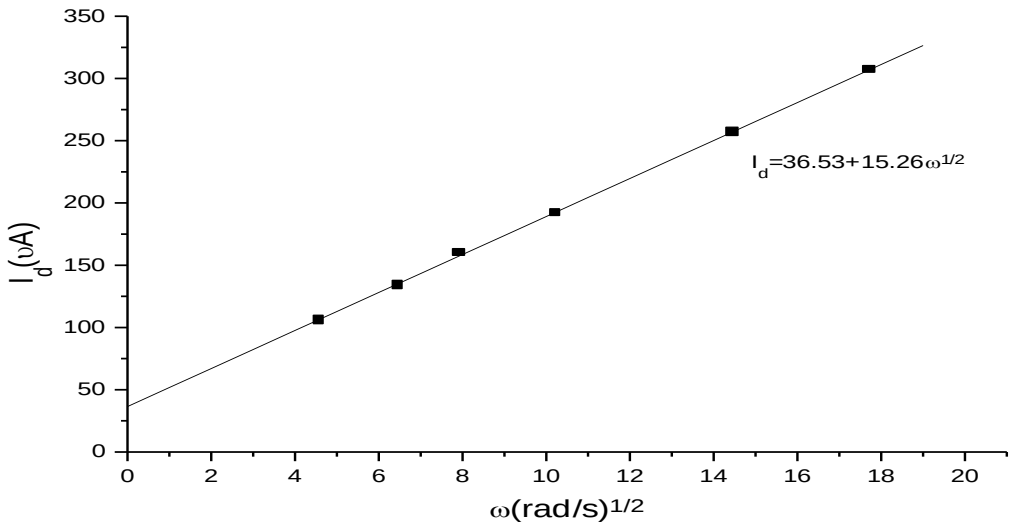

Figure 3. Variation in the limit diffusion current,according to the square root of rotation speed in 9g/L NaCl.

The expression of I_L depends on the speed of the electrode of pure iron. The process is a kinetic mixed. The current level is therefore characteristic of a diffusion phenomenon. More, the cathodic reaction involved in this corrosion system is reduced dissolved oxygen according to the reaction (1).

The values of the corrosion current density I_{corr}, obtained by Tafel extrapolation believe significantly with rotation speed. This increase is related to the decrease in the thickness of the diffusion layer when the speed increases. Figure 2 shows the progress and results obtained are summarized in Table 1.

Table 1. Electrochemical parameters of pure iron according to the rotation speed in 9g/L NaCl aerated at 310K.

rotational speed rd/min	E_{corr} (mV/SCE)	I_{corr} ($\mu A/cm^2$)	b_c (mV/dec)	I_L ($\mu A/cm^2$)
200	-580	23	60	135
400	-600	58	51	145
600	-580	65	61	200
1000	-520	80	61	235
2000	-530	98	61	320
3000	-540	113	58	366

Analysis of these results shows that the corrosion potential E_{corr}, evaluated towards higher values when the rotation speed increases. The values of the slopes show that it has no effect on the cathodic process. Indeed, all curves have the same allure cathode. Figure 3 shows no effect attributed to the rotation speed of the general shape of anodic curves. However, we note that there is a slight change in anodic current density in the range of potential from about -600 to -350 mV/SCE.

3.3. Comparative study of the effect of amino acid and amino esters.

Figure 4 shows the anodic and cathodic curves of pure iron in 9g/L NaCl aerated at 310K in the absence and presence of different inhibitors, at the concentration 10^{-2}M. The molecules studied are: MetOH, $MetOCH_3$, and MetOC2H5. The results obtained from IE curves are grouped in Table 2.

Analysis of these results can be noted that the addition of the products does not change the shape of the cathodic and anodic curves. The value of current density diffusion limit I_L practically unchanged. In the anodic domain, the addition of a product causes an increase in anodic currents. This increase is particularly pronounced in the presence of $MetOC_2H_5$ and $MetOCH_3$.

In the cathodic domain, we note that near the corrosion potential, cathodic currents decrease in the presence of the compounds. This decrease is more pronounced in the case of $MetOC_2H_5$. The added compounds displace also the corrosion potential towards more cathodic values. Inhibitory efficiency, determined from the corrosion current density, is defined by the following relation

$$E_I\,\% = \frac{I_{corr} - I'_{corr}}{I_{corr}} \times 100$$

I'_{corr} and I_{corr} represent the corrosion current densities in the medium, respectively with and without inhibitor, in identical experimental conditions.

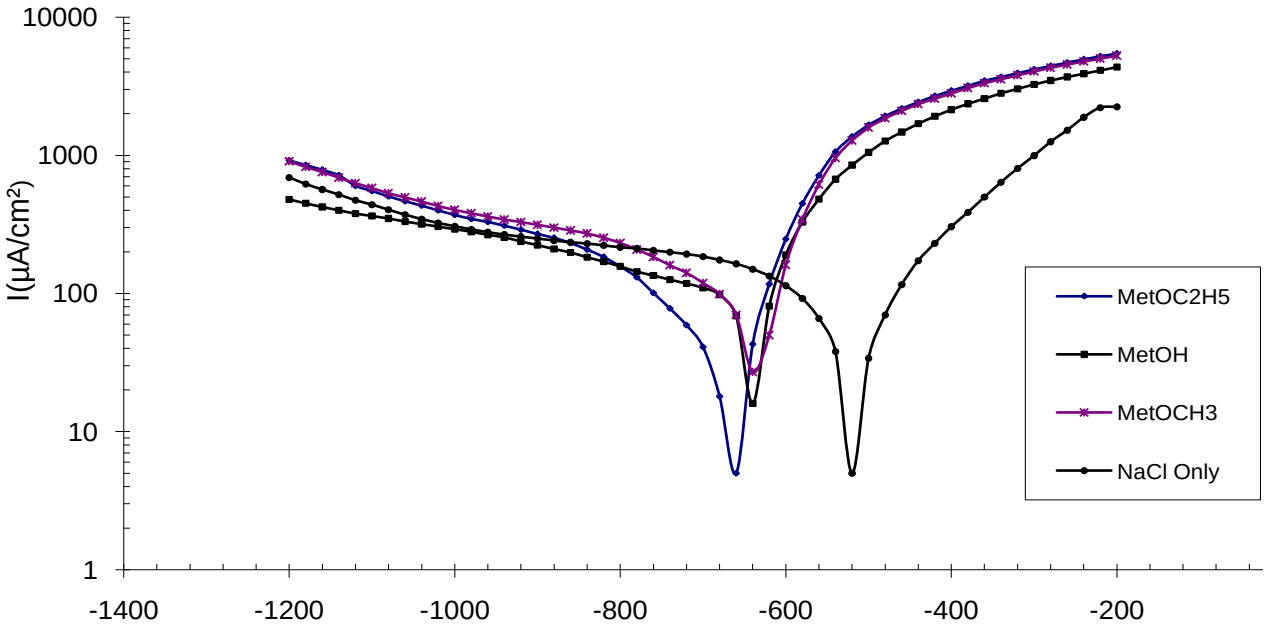

Figure 4. Anodic and cathodic polarization curves of pure iron in 0.9% NaCl medium aerated at 310K in the absence and presence of various compounds at 10^{-2}M.

Table 2 shows a decrease in corrosion current with all the inhibitors tested. The decrease ranges from MetOH (58µA/cm²) at $MetOC_2H_5$ (16µA/cm ²). The order of inhibitory efficiency can be established in the following order:

$$MetOC_2H_5 > MetOCH_3 > MetOH$$

Table 2. Electrochemical parameters of iron in 9 g / L NaCl with and without inhibitors at 10^{-2} M at 310 K.

inhibitor concentration	E_{corr} (mV/SCE)	I_{corr} (µA/cm^2)	b_c (mV/dec)	I_L (µA/cm^2)	E%
9 g / L NaCl	-540	80	61	235	-
10^{-2}M MetOH	-640	58	32	300	28
10^{-2}M $MetOCH_3$	-638	48	34	320	40
10^{-2}M $MetOC_2H_5$	-660	16	45	350	80

We note also, the $MetOC_2H_5$ is best inhibitors. The effectiveness reached 80% at 10^{-2}M. Inhibitory efficiency is improved by the substitution of Hydrogen atom by the donor groups, the methyl group (CH_3) or the ethyl group (C_2H_5). It passes, respectively, from 28% to 40% and 80%. Figure 5 shows the anodic and cathodic polarization curves of pure iron in 9g/L NaCl aerated in the absence and presence of $MetOC_2H_5$ at different concentrations, ranging from 10^{-5}M to 10^{-2}M.

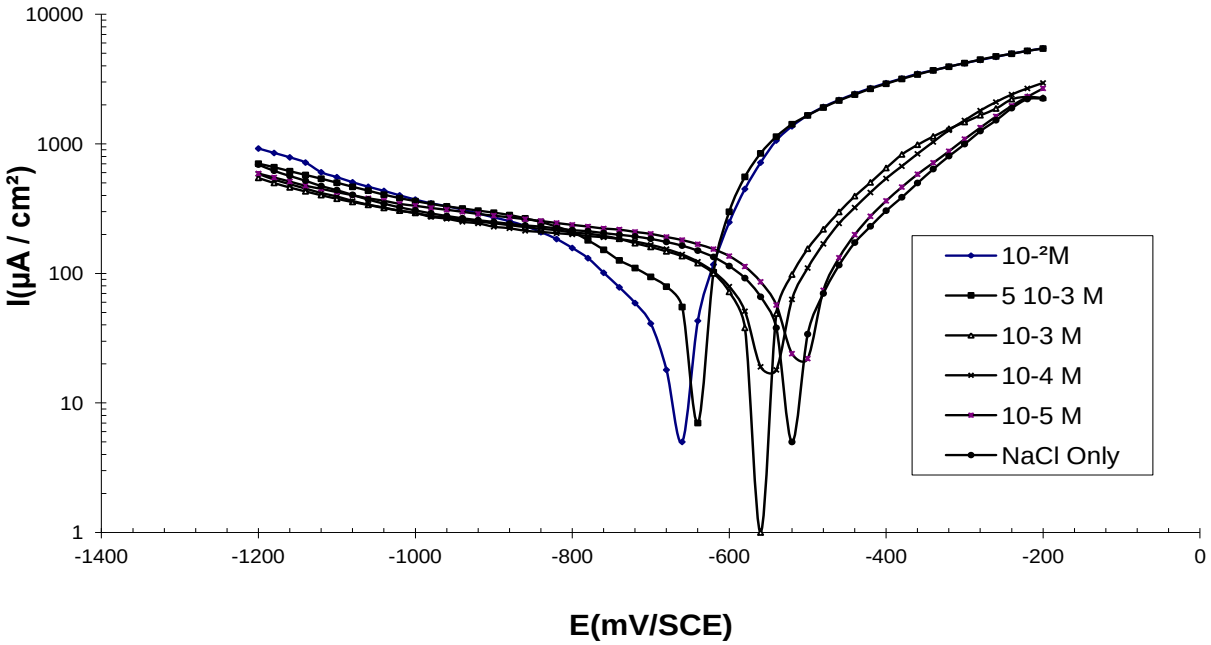

Figure 5. Anodic and cathodic polarization curves of pure iron in 9g/L NaCl aerated in the absence and presence of $MetOC_2H_5$ at different concentrations.

Examination of the polarization curves in the presence of the inhibitor, allowed us to make the following findings. The cathodic curves are displaced more towards the low values of current densities when the concentration of $MetOC_2H_5$ increases. We also noted a decrease in the cathodic current; this decrease is more pronounced between the corrosion potential and level of oxygen diffusion. This level becomes smaller where the concentration of $MetOC_2H_5$ increases and shifts to values more negative potentials.

This indicates retardation in the reduction of oxygen. The inhibitory effect is maximal for the concentration 10^{-2}M; the level diffusion is practically nonexistent.

The electrochemical parameters associated with these measurements are summarized in Table 3. The results show that the increase in concentration is accompanied by a decrease in the corrosion current density I_{corr} and an increase in efficiency inhibitory. It is important to note that a major leap in efficiency is observed when the inhibitory concentration $MetOC_2H_5$ goes from 5.10^{-3}M to 10^{-2}M. She spends 40% to 80%.

Table 3. Electrochemical Parameters in aerated 0.9% NaCl medium with and without addition of different concentrations of MetOC2H5 at 310K.

$MetOC_2H_5$	E_{corr} (mV/SCE)	I_{corr} (µA/cm²)	b_c (mV/dec)	I_L (µA/cm^2)	E%
Blanc	-540	80	61	235	-
10^{-5}M	-520	80	71	250	0
10^{-4}M	-550	64	67	220	20
10^{-3}M	-560	54	47	225	33
5.10^{-3}M	-640	48	50	305	40
10^{-2}M	-660	16	45	350	80

In the anodic domain, the curves follow the same shape. However, they are moved towards the high values of current with the increasing concentration of $MetOC_2H_5$ from 5.10^{-3}M. This result suggests that $MetOC_2H_5$ acts mainly as cathodic inhibitor

3.4. Effect of temperature

Temperature is one of factor that can affect the electrochemical behaviour of a metal in a corrosive environment. The metal-inhibitor interactions can also be influenced by this factor. The solutions studied were aerated, so having dissolved oxygen. An increase in temperature causes a release of oxygen. The concentration of dissolved oxygen decreases with increasing of temperature. And therefore the medium is devoid of oxygen to temperatures above 50 °C. On the other hand, the increase in temperature causes an increase in the diffusion speed. In order to interpret these phenomena, we conducted a study of the effect of temperature on the corrosion of pure iron in 9 g/L NaCl aerated. For this, we chose a temperature range between 22 and 60 °C to trace the polarization curves.

Figure 6 shows the polarization curves of pure iron in 9 g/L NaCl aerated at different temperatures. The results shows that increasing the temperature does not affect generally these curves, but causes an increase in cathodic and anodic currents even more pronounced in the anodic domain.

However, the figure 6 shows two distinct temperature domains. In the first interval [22-37 °C], the curves keep the overall look of the control curve, including the level diffusion cathodic whose height increases slightly. However, in the second interval [50-60 °C]; there is a marked reduction of the level diffusion without increasing its height. Note also that the cathodic current densities increase in the potential domain of -900 to -1200 mV / SCE, while they remain constant or decrease in the domain of potential on the level diffusion. We concluded that the impoverishment of dissolved oxygen in the solution after the temperature rise would be behind all these changes.

Table 5 shows the various parameters recorded, from anodic curves as a function of temperature. bc values do not change from 22 to 37 °C. We can therefore conclude that the electrochemical mechanism remains the same in the temperature domain. The corrosion current

density increases considerably with temperature; it goes from 22 μA/cm^2 at 32° C to 37 μA/cm^2 at 80 °C. The corrosion potential does not significantly changes as a function of temperature.

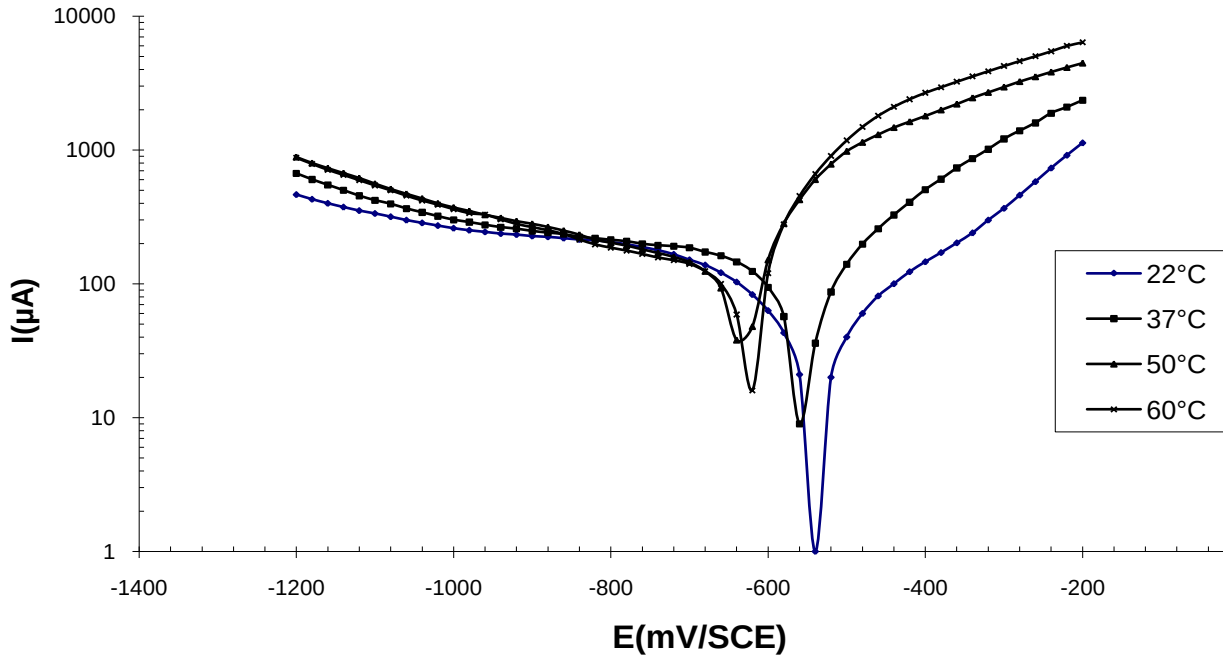

Figure 6. Polarization curves of pure iron in NaCl 9 ‰ medium at different temperatures

Table 5. Influence of temperature on the electrochemical parameters of pure iron in 9 g/L NaCl

T (°C)	E_{corr} (mV/SCE)	I_{corr} (μA/cm²)	b_c (mV/dec)	I_L (μA)
22	-540	32	52	215
37	-540	80	61	235
50	-639	129	60	-
60	-618	42	40	-

The influence of temperature on the inhibitor $MetOC_2H_5$ was also studied under the same conditions. The concentration chosen was 10^{-2}M in $MetOC_2H_5$, appears in Figure 7. The corresponding results are given in Table 6.

Table 6. Influence of temperature on the electrochemical parameters of pure iron in 0.9% NaCl aerated in the absence and presence of 10^{-2}M $MetOC_2H_5$

T (°C)	E_{corr} (mV/SCE)	I_{corr} (μA/cm²)	b_c (mV/dec)	I_L (μA/cm²)	E %
22	-660	64	43	224	60
37	-660	16	45	350	80
50	-700	32	53	-	-
60	-600	100	67	-	-

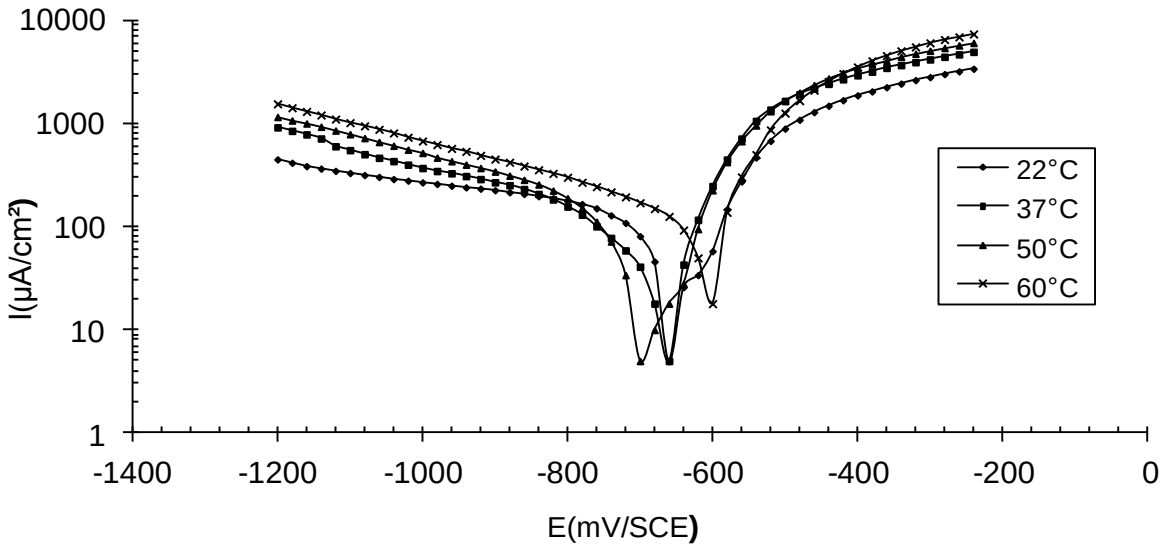

Figure 7. Polarization curves of pure iron in 0.9% NaCl, in the presence of 10^{-2} M $MetOC_2H_5$ at various temperatures.

The comparative study of these curves and data in the table 6, allows us to identify several findings. The values of corrosion current density decreases with increasing temperature to the threshold temperature of 50 ° C. beyond this value there is an increase in current density I_{corr}. Note also that the inhibitory efficacy increases with temperature from 60% to 22°C at 80% to 37 °C. We are also seeing a reduction in the level of diffusion, when the temperature increases up to almost disappear at 60 °C. This is due to the decrease in the concentration of oxygen dissolved in the medium, following the rise in temperature.

From the results obtained, we can note that the amino ester $MetOC_2H_5$ studied is a good inhibitor for iron in pure in 9 g / L NaCl. In the cathodic domain, the product is working without changing the mechanism of oxygen reduction. The comparative study of the corrosion inhibition indicates that the action of $MetOC_2H_5$ is more pronounced.

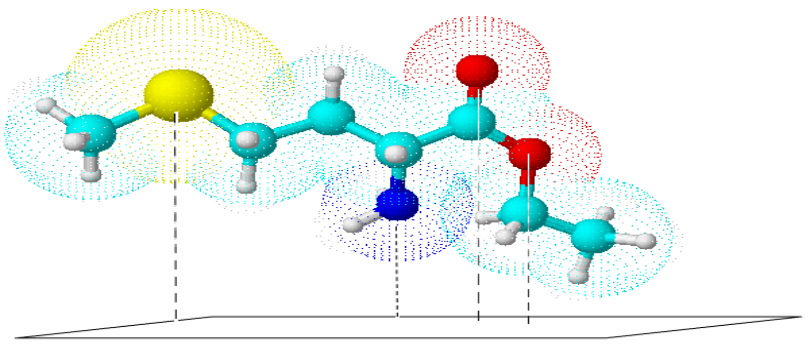

Scheme 3. The adsorption of the $MetOC_2H_5$ inhibitor on the surface of pure iron

This can be explained mainly by the presence of electron donating groups in the molecular structure of MetOC2H5. The adsorption of the inhibitor on the surface of pure iron is facilitated by the establishment of links such as "donor - acceptor." between the orbital ‘’d’’ unsaturated of iron and free doublets electrons of the atoms of sulfur and nitrogen, whose electro negativity is enhanced by the ethyl group, an electron donor. The adsorption is presented in schema 3:Inhibitor adsorbs on the pure iron surface according to the Frumkin kind isotherm model obeying to the relationship:

$$\left(\frac{\Theta}{1-\Theta}\right)\exp(-f\Theta)=\frac{1}{55.5}C.\exp\left(\frac{-\Delta G_{ads}}{RT}\right)$$

f is a function of adsorption energy and ΔGads is a standard free energy of adsorption

The S-shaped adsorption mode figure 8 indicates that the mechanism of inhibition involves the formation of double layer at the metal-solution interface. The shape of isotherm seems to reflect two modes of adsorption. At a very low concentration, the inhibitor adsorbate is either at the vertical mode or the all active sites on the surface are not partially occupied further increase of inhibitor concentration leads to the formation of multiplayer generally at horizontal mode.

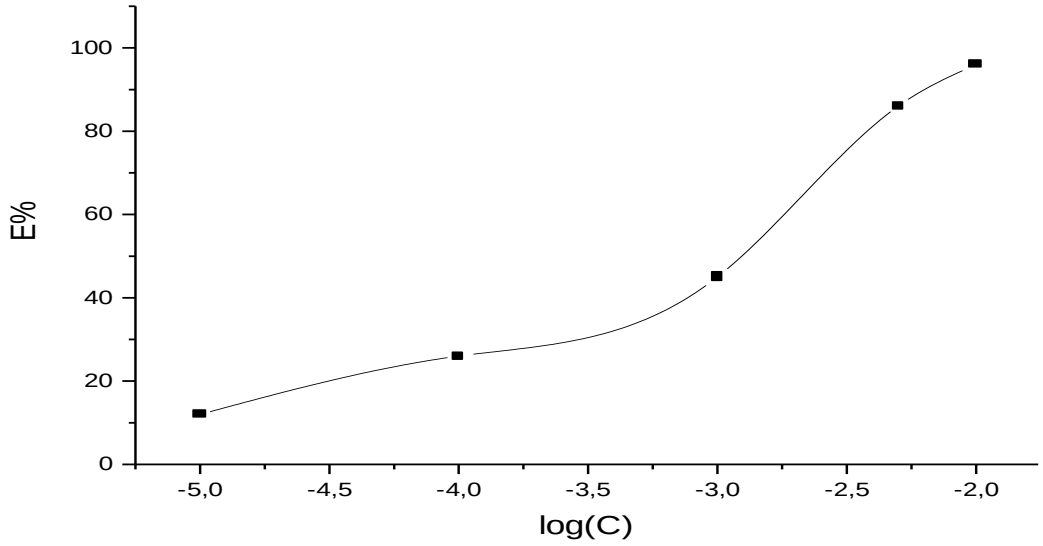

Figure 8. Frumkin isotherm for $MetOC_2H_5$ in 0.9% NaCl

4. CONCLUSION

The results allow making the following conclusions:

1 - The corrosion of pure iron in the medium 9 g / L NaCl following a mixed kinetics.

2 - Inhibitors tested show that methionine ethyl ester is the best in the series.

3 - The presence of the sulfur atom enhances the adsorption $MetOC_2H_5$ adsorption isotherm follows the Frumkin.

ACKNOWLEDGEMENTS
Prof S. S. Al-Deyab and Prof B. Hammouti extend their appreciation to the Deanship of Scientific Research at king Saud University for funding the work through the research group project.

References

1. D. Chicot, J. Mendoza, A. Zaoui, G. Louis, V. Lepingle, F. Roudet, J. Lesage, *Mater. Chem. Phys.*, 129 (2011) 862.
2. S. Kim, J. Surek, J. Baker-Jarvis, *Journal of Research of the National Institute of Standards and Technology*, 116 (2011) 655.
3. V.N. Rajakovic-Ognjanovic, D.Z. Zivojinovic, B.N. Grgur, L.V. Rajakovic, *Applied Thermal Engineering*, 31 (2011) 119.
4. T.J. Pan, H.T. Ma, Y.S. Li, *Corr. Eng. Sci. Technol.*, 46 (2011) 499.
5. N. Bertrand, C. Desgranges, D. Poquillon, M.C. Lafont, D. Monceau, *Oxidation of Metals*, 73 (2010) 139.
6. F. Gesmundo, F. Viani, *Mater. Chem. Phys*, 20 (1988) 513.
7. J. Weise, J. Baumeister, O. Yezerska, N. Salk, G.B.D. Silva, *Adv. Eng. Mater*, 12 (2010) 604.
8. E.M. Sherif, R.M. Erasmus, J.D. Comins, *Electrochimica Acta*, 55 (2010) 3657.
9. L. Caceres, T. Vargas, M. Parra, *Electrochimica Acta*, 54 (2009) 7435.
10. M. Olzon-Dionysio, S.D. de Souza, R.L.O. Basso, S. de Souza, *Surf. Coat. Technol.*, 202 (2008) 3607.
11. M. Guzman, R. Lara, L. Vera, *Journal of the Chilean Chemical Society*, 54 (2009) 123.
12. L. Caceres, T. Vargas, L. Herrera, *Corr. Sci.*, 49 (2007) 3168.
13. C.B. Santos, M. Metzner, C.F. Malfatti, J.Z. Ferreira, *Transactions of the Institute of Metal* Finishing, 87 (2009) 309.
14. M. Sahin, G. Gece, F. Karci, S. Bilgic, *J. Appl. Electrochem.*, 38 (2008) 809.
15. D. Wahyuningrum, S. Achmad, Y.M. Syah, Buchari, B. Bundjali, B. Ariwahjoedi, *Int. J. Electrochem. Sci.*, 3 (2008) 154.
16. V. Afshari, C. Dehghanian, *Mater. Chem. Phys*, 124 (2010) 466.
17. N.H. Helal, W.A. Badawy, *Electrochimica Acta*, 56 (2011) 6581.
18. Ranjana, R. Banerjee, M.M. Nandi, *Indian J. Chem.Technol.*, 17 (2010) 176.
19. M. Behpour, S.M. Ghoreishi, N. Mohammadi, M. Salavati-Niasari, *Corr. Sci*, 53 (2011) 3380.
20. M.A. Amin, K.F. Khaled, Q. Mohsen, H.A. Arida, *Corr. Sci*, 52 (2010) 1684.
21. Y.M. Tang, X.Y. Yang, W.Z. Yang, R. Wan, Y.Z. Chen, X.S. Yin, *Corr. Sci*, 52 (2010) 1801.
22. M.M. El-Rabiee, N.H. Helal, G.M.A. El-Hafez, W.A. Badawy, *J. Alloys Compounds*, 459 (2008) 466.
23. M.S. Morad, *J. Appl. Electrochem*, 38 (2008) 1509.
24. M. Dudukcu, *Materials and Corrosion-Werkstoffe Und Korrosion*, 62 (2011) 264.
25. A.Y. Musa, A.A.H. Kadhum, A.B. Mohamad, M.S. Takriff, A.R. Daud, S.K. Kamarudin, *Corr. Sci*, 52 (2010) 526.
26. M. Zerfaoui, B. Hammouti, H. Oudda, M. Benkaddour, S. Kertit, *Bull. Electrochem.*, 20 (2004) 433.
27. A.Chetouani, M. Daoudi, B. Hammouti, T. Ben Hadda, M. Benkaddour, *Corr. Sci*, 48 (2006) 2987.
28. Chetouani, B. Hammouti, T. Benhadda, M. Daoudi, *App. Surf. Sci.*, 249 (2005) 375.
29. Chetouani, K. Medjahed, K.E. Sid-Lakhdar, B. Hammouti, M. Benkaddour, A. Mansri, *Corr. Sci.*, 46 (2004) 2421.
30. Chetouani, B. Hammouti, A. Aouniti, N. Benchat, T. Benhadda, *Progress in Organic Coatings*, 45 (2002) 373.
31. H. Bhandari, V. Choudhary, S.K. Dhawan, *Synthetic Metals*, 161 (2011) 753.

32. O.K. Abiola, M.O. John, P.O. Asekunowo, P.C. Okafor, O.O. James, *Green Chemistry Letters and Reviews*, 4 (2011) 273.
33. N.O. Eddy, F.E. Awe, C.E. Gimba, N.O. Ibisi, E.E. Ebenso, *Int. J. Electrochem. Sci.*, 6 (2011) 931.
34. S. Ahn, H.J. Song, J.W. Park, J.H. Lee, I.Y. Lee, K.R. Jang, *Korean Journal of Chemical Engineering*, 27 (2010) 1576.
35. M. Lashgari, M.R. Arshadi, M. Biglar, *Journal of the Iranian Chemical Society*, 7 (2010) 478.
36. L. Liu, Y. Li, F.H. Wang, *J. Mater. Sci. Technol.*, 26 (2010) 1.
37. H. Nanjo, Y. Suzuki, J. Hayasaka, F.M.B. Hassan, S. Venkatachalam, M. Nishioka, M. Kanakubo, T. Aida, J. Onagawa, *Electrochimica Acta*, 55 (2010) 4685.
38. G.S. Was, S. Teysseyre, Z. Jiao, *Corrosion*, 62 (2006) 989.
39. E.J. Reardon, R. Fagan, J.L. Vogan, A. Przepiora, *Environ. Sci. Technol.*, 42 (2008) 2420.
40. K. Es-Salah, M. Keddam, K. Rahmouni, A. Srhiri, H. Takenouti, *Electrochimica Acta*, 49 (2004) 2771